

# Active Pixel Sensor (APS) based Star Tracker

Dr. Carl Christian Liebe  
E-mail: [earl.c.licbc@jpl.nasa.gov](mailto:earl.c.licbc@jpl.nasa.gov)  
Telephone: 818-354-7837

Dr. Edwin W. Dennison  
E-mail: [edwin.w.dennison@jpl.nasa.gov](mailto:edwin.w.dennison@jpl.nasa.gov)  
Telephone: 8183546074

Dr. Bruce Hancock  
E-mail: [bruce.r.hancock@jpl.nasa.gov](mailto:bruce.r.hancock@jpl.nasa.gov)  
Telephone: 8183548801

Dr. Robert C. Stirbl  
E-mail: [robert.c.stirbl@jpl.nasa.gov](mailto:robert.c.stirbl@jpl.nasa.gov)  
Telephone: 8183545436

Dr. Bedabrata Pain  
E-mail: [bedabrata.pain@jpl.nasa.gov](mailto:bedabrata.pain@jpl.nasa.gov)  
Telephone: 8183540614

Jet Propulsion laboratory, California Institute of Technology,  
4800 Oak Grove Dr, Pasadena CA 91109-8099.

*Abstract* — Charge-Coupled Device (CCD) based star trackers provide reliable attitude estimation onboard most 3 axis stabilized spacecraft. The spacecraft attitude is calculated based on observed positions of stars, which are located and identified in a CCD image of the sky.

A new photon sensitive imaging array - Active Pixel Sensors (APS) - has emerged as a potential replacement to CCDs. The APS chips utilize existing Complementary Metal Oxide Semiconductor (CMOS) production facilities, and the technology has several advantages over CCD technology. These include: lower power consumption, higher dynamic range, higher blooming threshold, individual pixel readout, single 3.3 or 5 Volt operation, the capability to integrate on-chip timing, control, windowing, Analog to Digital (A/D) conversion anti centroiding operations. However, because the photosensitivity of an APS pixel is non-homogeneous, its suitability as a star tracker imager has been unknown.

This paper reports test results of a 256 x 256-pixel APS chip for star tracker applications. Using photon transfer curves, a system read-out noise of 7 electrons, under laboratory conditions, has been determined (photogate type). The full well of an APS pixel is determined to be around 450,000 electrons. Utilizing astronomical observations, the sensitivity of APS was measured to  $13600 \text{ e}^-/(\text{second}\cdot\text{mm}^2)$  for a 0<sup>th</sup> magnitude star. Centroiding accuracy of the APS was in the order of 1/10 pixel. The dynamic range of the APS was better than 9 magnitudes.

These measurements allow us to conclude that the APS is a potential replacement for CCD star trackers.

## TABLE OF CONTENTS

1. INTRODUCTION
2. APS TECHNOLOGY
3. LABORATORY MEASUREMENTS
4. ASTRONOMICAL MEASUREMENTS
5. SUMMARY
6. ACKNOWLEDGEMENTS
7. REFERENCES
8. BIOGRAPHIES

## 1. INTRODUCTION

Typically the attitude of a 3 axis stabilized spacecraft is determined by a star tracker. A star tracker is an electronic camera connected to a microcomputer. Using a sensed image of a portion of the sky, stars can be located and identified. Thus the orientation of the spacecraft can be determined based on these observations. A modern star tracker is fully autonomous - i.e. it automatically performs pattern recognition of the star constellations in the field of view and calculates the attitude quaternion with respect to the celestial sphere, see figure 1 [1], [2]. State of the art star trackers utilize CCD imagers.<sup>1</sup> They typically have a mass of 1-7 kg and consume 5-12 watts of power. Their accuracy is in the arc seconds range [3].

<sup>1</sup> Such as the Lockheed Martin missile Systems AST201 or the Technical University of Denmark ASC or the Computer Resources International 15-AS or the Daimler-Benz Aerospace Jena-Optronik SETIS.

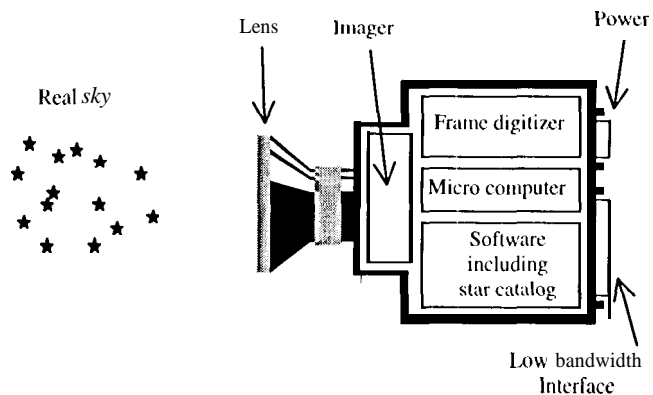


**Figure 1.** Sketch of a modern star tracker.

The motivation for a replacement to the mature CCD technology is:

- **Simplified hardware:** A conventional CCD chip requires different voltages and complicated waveforms to operate. Typically, 1/3-1 Watt is required to drive a CCD chip, including several supporting chips. APS chips operate on a single 3.3 or 5-volt supply. They consume an insignificant amount of power and require no special supporting chips. In addition, it is possible to implement an onboard A/D converter, which facilitates a direct communication line to a microcomputer/microcontroller. This will be significant to the construction of star trackers for future micro spacecraft and probes where power consumption and mass are critical.
- **No blooming:** Most autonomous star trackers do not operate well when there are bright objects present in the field of view due to blooming on the CCD chip. This phenomenon significantly decreases the sky coverage for earth orbiting star trackers. Future National Aeronautics & Space Administration (NASA) missions that plan to utilize an autonomous star tracker during close encounters with solar system bodies will have to operate with an extended body in the field of view. The blooming problem is eliminated with an APS based star tracker.
- **More radiation resistant:** APS technology will probably be better suited for high radiation missions than CCD technology in the future [4]. The largest advantage of APS is that the pixels are addressed directly, so the Charge Transfer Efficiency (CTE) degradation that affects CCDs subjected to proton irradiation is eliminated.

At present, APS chips suffer an increase in dark current with ionizing dose comparable to that seen in conventional (non-Multi-finned Phase (MPP)) CCDs. However, it is believed that the use of pinned photodiodes will eliminate this problem, just as the corresponding MPP technology has done for CCDs. The residual component of dark current due to

displacement damage from protons can not be eliminated, but is expected to be similar to or less than that in MPP CCDs. In any case, cooling can mitigate dark current problems.

The use of commercially available radiation hard processes, which is already underway, should also offer improvements, including the elimination of latchup and minimization of Single Event Upsets (SEU).

To determine if current APS technology is suitable for a star tracker, parameters specific to star tracking (e.g. absolute sensitivity and sub-pixel accuracy) have been investigated. The evaluation was based on a 256x256 pixel Jet Propulsion Laboratory (JPL) designed APS chip. The APS chip itself was mounted in a vacuum chamber to cool it without condensation. Also, a rudimentary support circuit for transferring the image to a PC was constructed. The setup is depicted in figure 2.

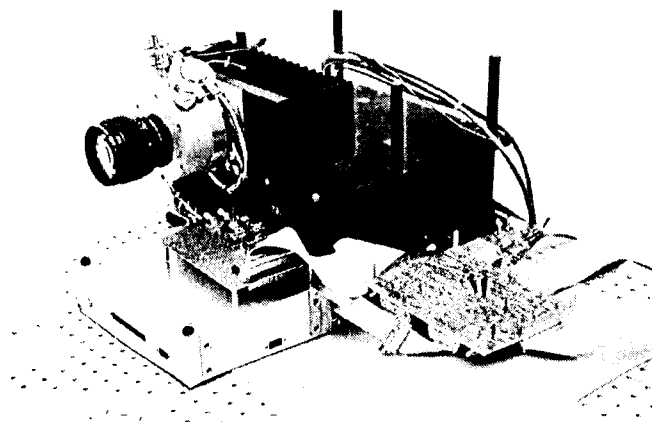


**Figure 2.** The APS setup.

The noise and the full well capacity of an APS pixel were determined in a laboratory at JPL. The evaluation of the absolute light sensitivity and the sub-pixel accuracy was performed at Table Mountain Observatory, Wrightwood, CA.

## 2. APS TECHNOLOGY

An active pixel sensor is an imaging array with active transistors located with each pixel. Two types of APSS exist: photo diode pixel and photo gate pixel. The tested APS is a 20.4  $\mu\text{m}$  photo diode pixel with 3 transistors per pixel. Typical pixel pitch is  $\sim 17\times$  the minimum feature size [5]-[11]. The sensors are fabricated in a standard CMOS process. The Hewlett-Packard 1.2  $\mu\text{m}$  N-well CMOS process was provided through the MOSIS<sup>2</sup> service. The specific chip had a geometric fill factor of 32.570. The conversion factor is approximately 3 pV/electron.

<sup>2</sup>MOSIS aggregates designs from different sources onto one mask set, allowing designers to obtain small quantities and to share the cost of fabrication among a number of users.

The power consumption of Very Large Scale Integration (VLSI) CMOS is intrinsically low, and locating the CMOS circuits for timing and control on chip eliminates high power chip to chip communication. The power consumption is typically in the 20 mW range. Also, the CMOS will operate on a single 5 or 3.3 Volt supply.

Advancements in VLSI technology are easily incorporated onto a new APS. This includes the ability to provide additional functionality on a single chip (e.g. A/D conversion or potentially star centroid calculation). Examples of state-of-the-art APS miniature cameras are depicted in figure 3.

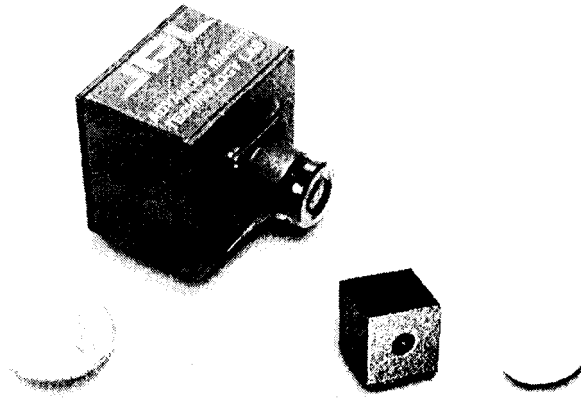


Figure 3. State-of-the-art APS miniature cameras, depicted with coins for comparisons.

### 3. LABORATORY MEASUREMENTS

When characterizing an imaging device, it is important to determine how many photoelectrons equals one A/D converter Digital Number (DN), the number of photoelectrons in a full well and the number of electrons in the system read-out noise. One way to determine this empirically is to utilize photon transfer curves [12]. A photon transfer curve, is an XY scatter plot of average pixel values and temporal pixel variations. The setup for making a photon transfer curve is depicted in figure 4.

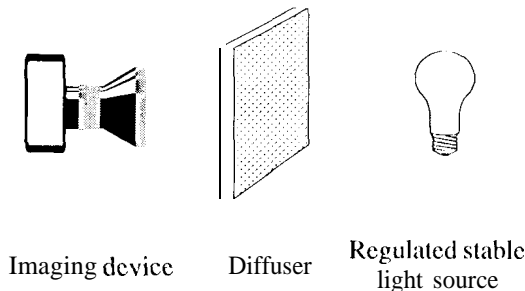


Figure 4. Photon transfer curve setup.

After acquiring two similar and homogeneous illuminated images (or smaller windows in the two images), with a given exposure time, the two images (image<sub>1</sub> and image<sub>2</sub>, each with dimension N<sub>x</sub> times N<sub>y</sub>) are subtracted from each

other pixel-wise to minimize the individual pixel variations. The temporal pixel variations are defined as:

$$V = \frac{\sum_{i=1}^{N_x} \sum_{j=1}^{N_y} (image_1(i, j) - image_2(i, j))^2}{N_x \cdot N_y - 1} \quad (1)$$

The average of the images is calculated as:

$$image = \frac{1}{2N_x N_y} \left( \sum_{i=1}^{N_x} \sum_{j=1}^{N_y} image_1(i, j) + \sum_{i=1}^{N_x} \sum_{j=1}^{N_y} image_2(i, j) \right) \quad (2)$$

The mean DN is shown as a function of exposure time in figure 5.

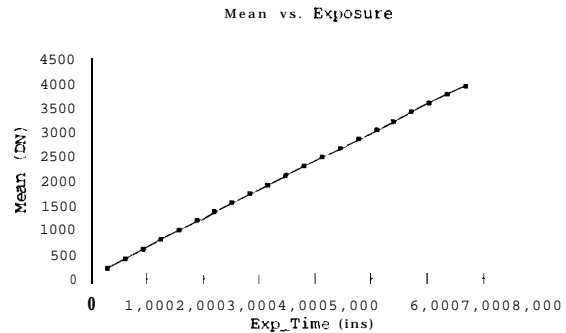


Figure 5. The mean DN as a function of the exposure times.

The average DN's and the temporal pixel variations are also measured for multiple average DN's, and the values are displayed in a XY scatter plot. This is the actual photon transfer curve. The photon transfer curve for the APS setup is displayed in figure 6.

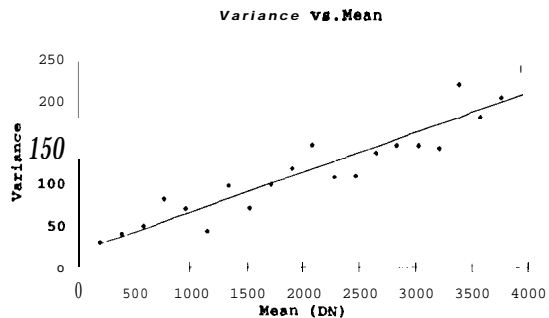


Figure 6. The measured photon transfer curve for the APS camera setup.

It is assumed that the measured signal in DN's is proportional to the number of photoelectrons, i.e.:

$$S_{converter} = x \cdot N_{Photoelectrons} \quad (3)$$

The signal noise, can then be expressed as (assuming the electronics do not generate noise independently):

$$\sigma_{signal} = x \sqrt{N_{Photoelectrons}} \quad (4)$$

$$\sigma_{Signal}^2 = \lambda \hat{N}_{Photoelectron} \quad (5)$$

Substituting the two equations yields:

$$\sigma_{Signal}^2 = x S_{Converter} \quad (6)$$

**Also, noise independent of the signal (readout noise) has to be added:**

$$\sigma_{Signal}^2 = x S_{Converter} + \sigma_{readout}^2 \quad (7)$$

This means that the unknown x, is the slope of the photon transfer curve. **Also,** 1/slope is equal the number of photoelectrons per DN. In the photon transfer curve as displayed in figure 6, the slope of the line is -0.048, which is equivalent of 20.77 electrons/DN.

The mean value corresponding to 0 second exposure time is (figure 5) equivalent to 45.06 DN. 45.06 DN has a variance on 20.34 (figure 6) or standard deviation (square root) on 4.51 DN. This is equivalent to 4.51 DN \* 20.77 electrons/DN = 94 electrons read-noise.

It must be emphasized that the amplifier and signal chain as displayed in figure 2 is rudimentary. The readout noise would be much better if an optimized circuit was utilized. Another test setup at **JPL** reports readout noise as low as 7 electrons. However, this is using a photogate type **APS**.

Photon transfer curves can also determine the full well of a pixel. In figures 7 and 8, the Signal **DN is** displayed as a function of the exposure time and the corresponding photon transfer curve. It is emphasized that the setup was changed for these measurements, so that the analog amplifier gain was much lower for these measurements.

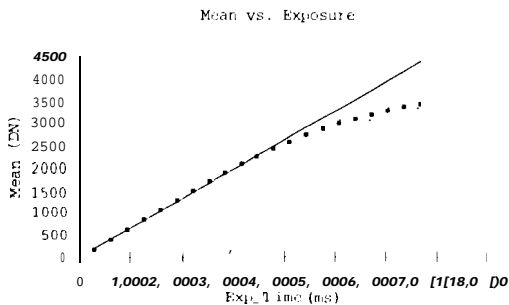


**Figure 7.** The mean DN as a function of the exposure times,

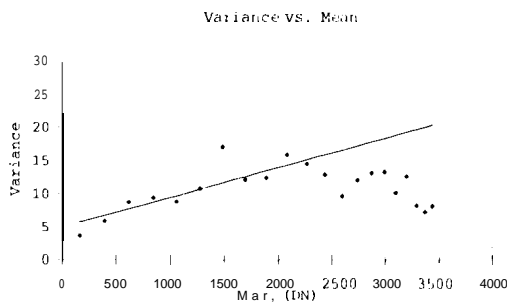


**Figure 8.** The measured photon transfer curve for the APS camera setup.

It is observed in figure 7, that the curve begins to deviate from a straight line around DN=2000. This is where the pixel response reaches non-linearity. The slope of the line in figure 8 (until DN=2000) is approximately 0.0044, which is equivalent to -225 photo electrons/DN. Full well is then 225 \* 2000 = 450,000 photoelectrons. This is higher than CCDs.

#### 4. ASTRONOMICAL MEASUREMENTS

For star tracker applications, it is essential to accurately determine the position of a star using sub-pixel accuracy<sup>3</sup>. It has been unclear whether APS pixels will support accurate sub-pixel calculations due to their pixel non-homogeneity.

The issue has been thoroughly investigated. The **APS** camera was taken to the **JPL** operated Table Mountain Observatory in Wrightwood, CA. The APS camera was mounted on a 24" telescope, which was used as a pointing device. By commanding the telescope to slew the night sky near zenith (to minimize atmospheric perturbation) it is possible to get multiple samples of a star within one pixel. For the setup, a commercial 50mm f/1.8 Canon photography lens was utilized. The field of view covered an inscribed circle with a diameter of -5.5°. The 24-inch telescope is depicted in figure 9.

<sup>3</sup> In a star tracker image, the image is defocused on purpose. This result in a star will be smeared out over a couple of pixels, the position of the star is calculated as the center of light (centroid) based on several pixels, Resolutions down to 1/100 of a pixel have been reported.

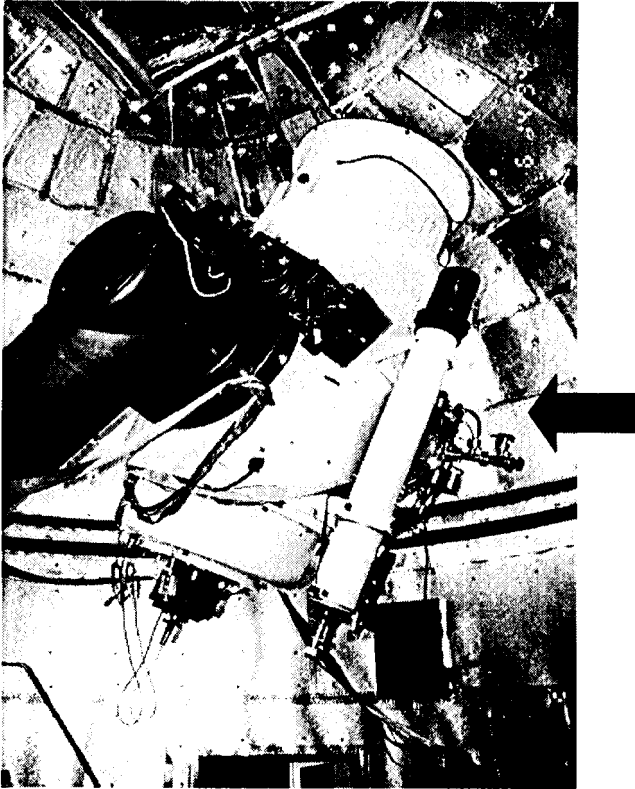


Figure 9. The APS setup mounted on a 24-inch telescope at Table Mountain Observatory, Wrightwood, CA. The black arrow identifies the APS camera. The plumbing is an ion-pump to evacuate the APS chip.

### Star Centroid Determination

To determine the suitability of the APS chip as a star tracker, an estimate of the accuracy in locating stars is needed. For this purpose, the algorithm described in the next paragraphs is used to locate stars in the image:

The image is sifted for pixels that are above a given threshold. Once a pixel is detected, a region of interest (ROI) window is aligned with the detected pixel in the center. The average pixel value on the border is calculated (see figure 10) and subtracted from all pixels in the ROI.

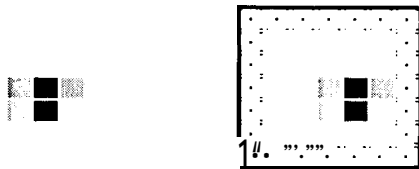


Figure 10. The region of interest (ROI), and the border of the ROI of a detected star.

The centroid and DN are calculated from the background-subtracted pixels in the ROI.

$$DN = \sum_{i=ROIstart}^{ROIend} \sum_{j=ROIstart}^{ROIend} image(i, j) \quad (8)$$

$$x_{cm} = \frac{\sum_{i=ROIstart}^{ROIend} \sum_{j=ROIstart}^{ROIend} i \cdot image(i, j)}{DN} \quad (9)$$

$$y_{cm} = \frac{\sum_{i=ROIstart}^{ROIend} \sum_{j=ROIstart}^{ROIend} j \cdot image(i, j)}{DN} \quad (10)$$

The centroid of a typically star during telescope tracking is displayed in figure 11.

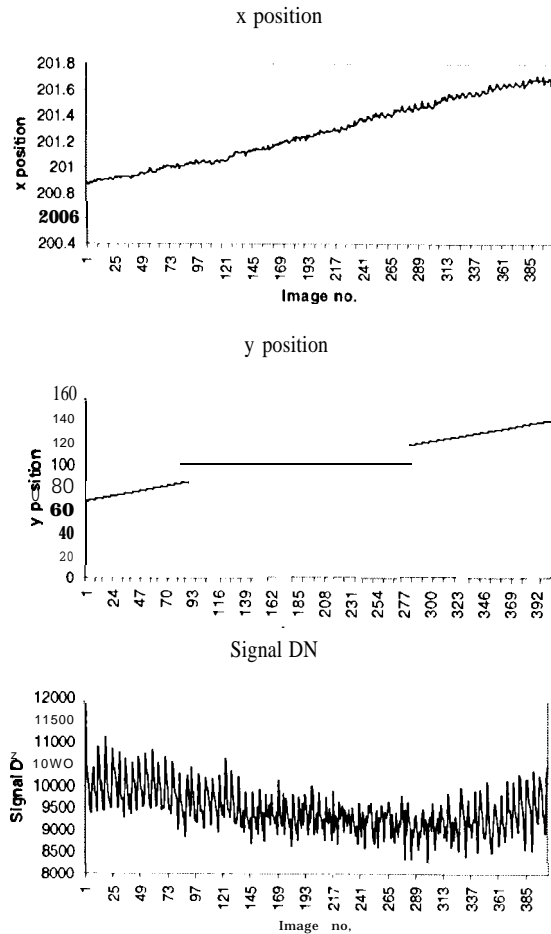


Figure 11. The centroid position and the DN for a typical star.

### Sub-pixel accuracy determination

Assuming that the telescope is moving in a straight path, it is possible to subtract the motion of the telescope and measure the residual<sup>4</sup>. To illustrate this, a scenario is depicted in figure 12. The telescope is moving in a straight path over the APS focal plane. The detected star centroids are not completely coincident with the real position. A line

<sup>4</sup>The residual is defined as the distance between the measured star position and the real star position,

(the residual) is drawn between the telescope position and the detected star centroid.

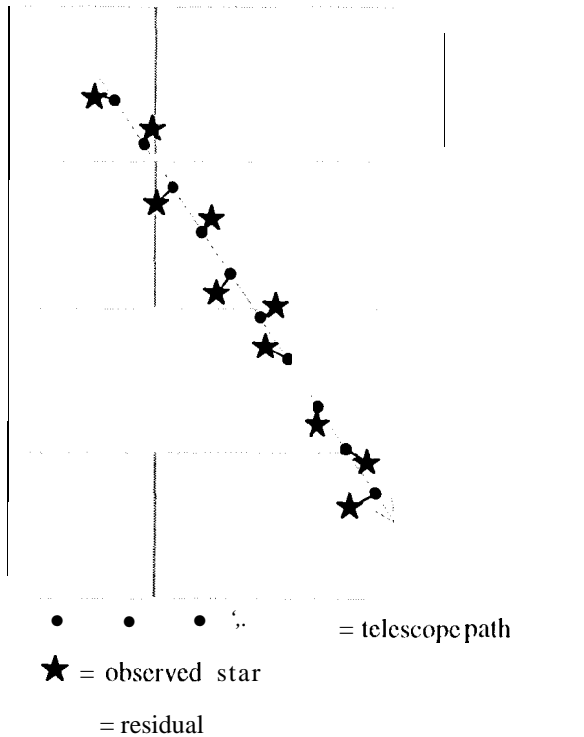


**Figure 12.** Illustration of the sub-pixel measurement. The figure covers an area on 4x4 pixels.

The result of subtracting the telescope motion from the star centroid positions in figure 11 is shown in figure 13.

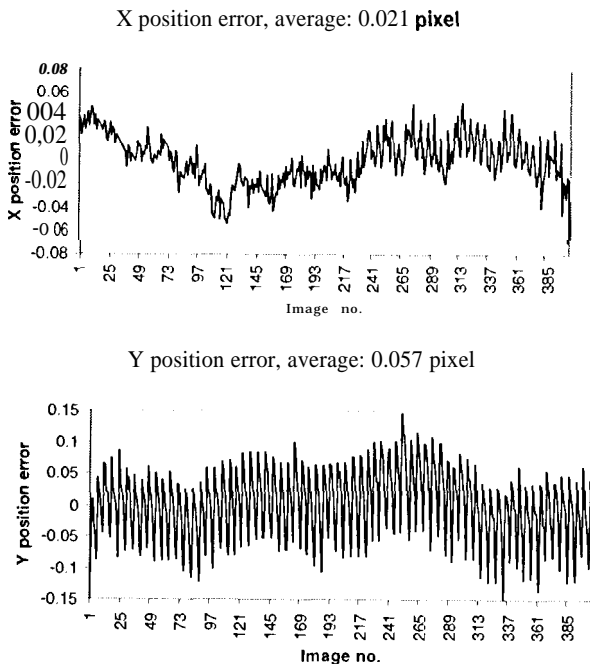


**Figure 13.** The centroiding residual.

The accuracy of the centroiding has been determined for many stars of different types. Typical accuracy is displayed in table I of the y position (the slew direction).

**Table 1.** Typical residuals for different stars.

Star	Residual (in pixels)	Average DN
Star 1 (faint)	0.177	900
Star 2 (bright)	0.046	21000
Star 3 (faint)	0.090	1750
Star 4 (bright)	0.048	20000
Star 5 (faint)	0.098	1500
Star 6 (bright)	0.037	19000
Star 7 (faint)	0.139	1000
Star 8 (bright)	0.057	13000

As observed in table 1, the APS is able to determine the centroid of a star to approximately 1/10 of a pixel. In the case that the star is very faint, the centroiding accuracy is worse than 1/10 pixel. This is comparable to a conventional CCD chip.

### Light Sensitivity

The absolute light sensitivity of an APS chip is also very important, when utilized in star tracker applications. The APS chip has higher quantum efficiency than CCD chips, but it also has lower geometric fill-factor, and the micro lens solution used in some CCD's have not yet been produced for APS chips.

To determine the light sensitivity, a star image was acquired and identified manually using a star catalog. The measured DN was normalized for magnitude, pupil area, exposure time, and electrons/IDN. The star image is displayed in figure 14, and the magnitude measurements are displayed in table 2.

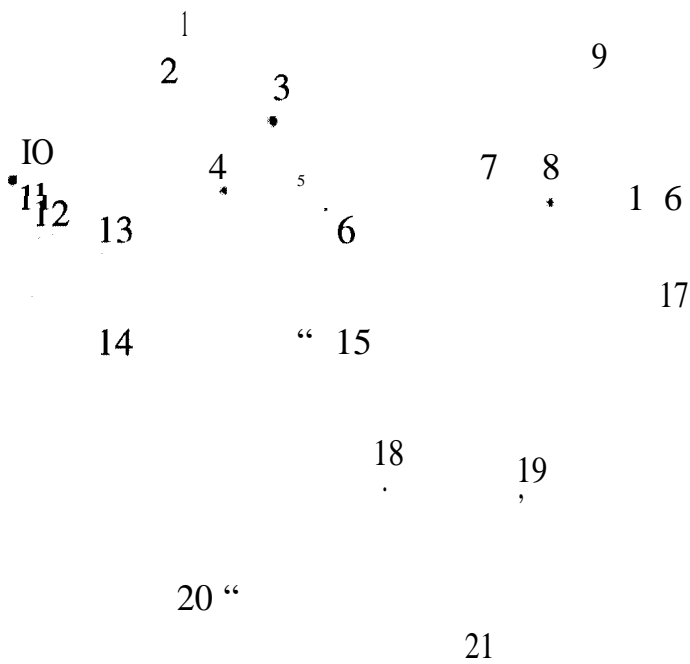


**Figure 14.** A star image acquired with the APS chip. Field of view is 5.5°. Exposure time is 3.06 Seconds. The F/no is 1.8. The numbers refer to the identified stars. For reproduction purposes the image contrast has been enhanced.

In the setup the gain of the amplifier was set to 30 electrons/DN. The exposure time was 3.06 seconds, and the lens was 50-111111 focal length and F/no 1.8, i.e. the aperture of the lens was 27.8 mm and the pupil area was 2428 mm<sup>2</sup>. A normalized sensitivity of the APS chip is defined as (for a magnitude 0 star):

$$Sensitivity = \frac{Signal\ DN \cdot \frac{e^-}{DN} \cdot 2.5^{M_v} \cdot 4}{T_{Exposure} \cdot Aperture^2 \cdot \pi} \quad (11)$$

The conclusion based on table 2 is that the average normalized sensitivity is ~13600 e<sup>-</sup>/(seconds\*mm<sup>2</sup>) for a magnitude 0 star, which is comparable to CCDs.

#### Dynamic range

There is a large span of magnitudes that can be encountered during astronomical observations. In star tracker applications, the system will typically be adjusted to detect as much light as possible for detecting many faint stars. A CCD chip will tend to bloom, if there is a bright object in the image (e.g., a planet, the moon). To explore this effect, an image with a bright planet (Mars) was acquired with 30 seconds exposure time to determine if the planet was blooming and if it was possible to detect faint stars at the same time. The result is displayed in figure 15.

It is observed that faint stars of 8<sup>th</sup> magnitude can readily be detected close to Mars, which approximately had magnitude -1 at the time. This is a huge dynamic non-blooming range.

The reason that stars fainter than 8<sup>th</sup> magnitude are not detected is due to the dark current, as the chip had an operating temperature on -0.5°C to 0.5°C. This is typical for a star tracker application with passive cooling.

#### 5. SUMMARY

This paper reports how APS technology will perform when utilized for star tracker applications. In a laboratory setup, the readout noise of the APS chip was determined to be 94 electrons (though as low as 7 have been reported, for photogate type APS chips). The full well of the APS pixel is approximately 450,000 electrons. The achievable sub-pixel accuracy was approximately 1/10 pixel and the absolute sensitivity was comparable to CCD chips. The overall conclusion is that the APS technology can be utilized in star tracker applications, with similar performance to that of CCD's. However, lower power consumption, simplified operation, larger dynamic range and potentially better radiation robustness are the strengths of the APS technology.

#### 6. ACKNOWLEDGEMENTS

The authors will like to thank Dr. Suraphol Udomkesmalee and Curtis Padgett of JPL for valuable comments during writing of this paper.

The research described here was carried out at the Jet Propulsion Laboratory, California Institute of Technology, and was sponsored by the National Aeronautics and Space Administration. References herein to any specific commercial product, process or service by trademark, manufacturer, or otherwise, does not constitute or imply its endorsement by the United States Government or the Jet Propulsion Laboratory, California Institute of Technology.

#### 7. REFERENCES

- [1] C. C. Liebe: Pattern recognition of Star Constellations for spacecraft applications, *IEEE AES Magazine*, p.31-39, 1993.
- [2] C. C. Liebe: Star Trackers for attitude determination, *IEEE Aerospace and Electronics Systems Magazine*, p. 10-16, June 1995.
- [3] A. R. Eisenman, C. C. Liebe, J. L. Joergensen: The new generation of autonomous star trackers, *Europto, SPIE, London*, September 1997.
- [4] Bruce Hancock, Radiation Effects in CCD and APS Sensors, A Comparative Overview, 7/31/97, presentation at JPL, Internal document.
- [5] S. K. Mendis et al: CMOS Active Pixel Image Sensors for Highly Integrated Imaging Systems, *IEEE Journal of Solid State Circuits*, Vol. 32, No. 2, February 1997.
- [6] R. H. Nixon et al: 128x128 CMOS Photodiode-type active pixel sensor with on-chip timing, control and signal electron optics, *Proceedings of the SPIE* vol. 2415, *Charge-Coupled Devices and Solid State Optical Sensors V*, paper 34 (1995).
- [7] C.C. Clark et al: Applications of APS array to star and feature tracking systems, *Proc. of SPIE*, Vol. 26'10, p. 116-120, Denver 1996.

**Table 2.** Normalized sensitivity for different stars (NA = not available)

No.	Signal DN	Class	$M_V$	$M_B$	Sensitivity $e/(\text{sec} * \text{mm}^2)$	Remark
1	1959	K0	6.7	7.6	14624	Ok
2	1600	B9	6.9	6.9	14346	Ok
3	24391	NA	3.4	4.1		Overflow
4	I 1743	A0	4.4	4.3		Overflow
5	3865	A2	6.1	6.3	16650	Ok
6	I 407	A0	7.8	7.2	28777	Ok
7	1632	G5	NA	NA		Close star catalog star
8	13073	A()	4.2	4.2	9875	Ok
9	3944	F5/na	NA	NA		Close star catalog star
10	20722	K0	3.1	4.1		Overflow
11	1496	K2	6.7	8.0	11167	Ok
12	1617	KS	7.6	8.6		Close hot spot
13	2172	A3	6.3	6.4	11238	Ok
14	1174	A2	NA	NA		Magnitude NA
15	2054	B8	6.4	6.3	11648	Ok
16	2322	K5	6.9	8.0	20820	Ok
17	3329	K0	5.9	6.9	11939	Ok
18	I 1773	B3	4.3	4.1	9747	Ok
19	10564	K0	4.5	5.6	10505	Ok
20	1199	G5	7.3	8.0	15510	Ok
21	1698	K2	6.8	8.0	13892	Ok

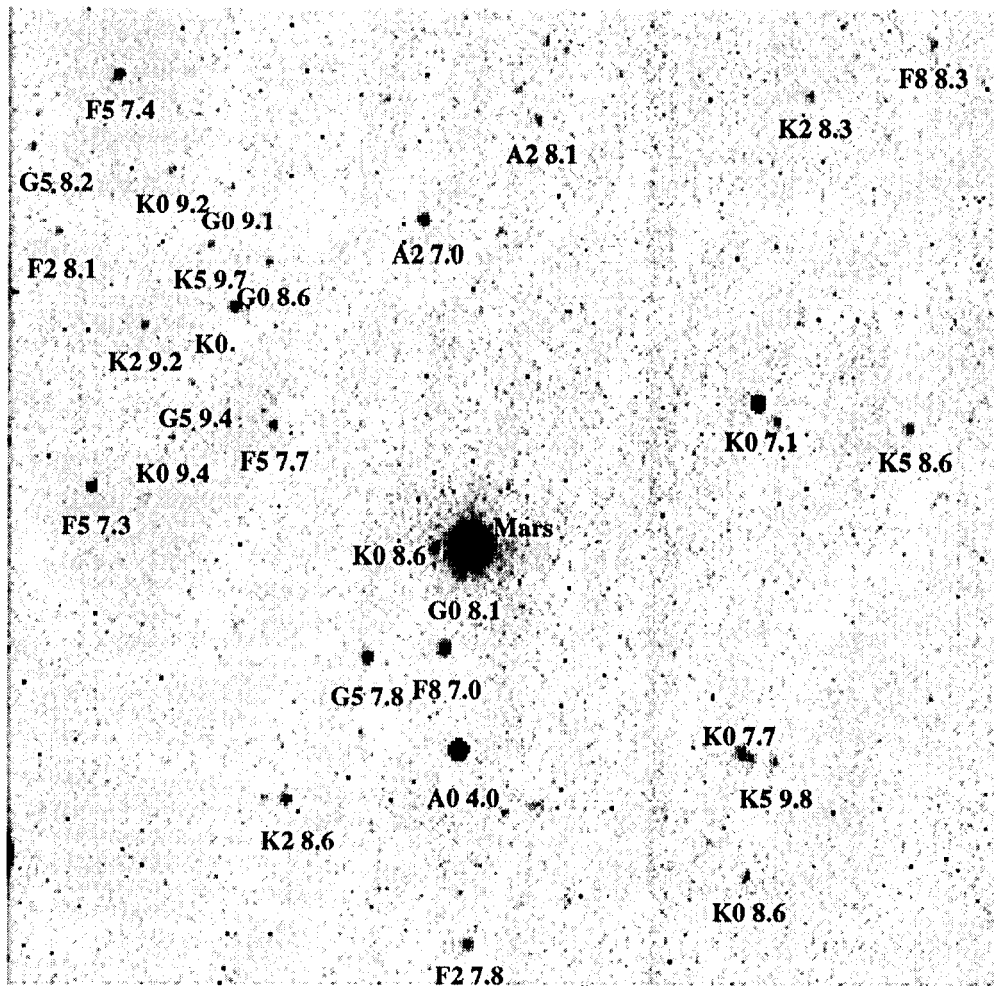


**Figure 15.** Mars in the center of the image. Stars down to 8<sup>th</sup> magnitude are readily detected simultaneously.

[8] O. Yadid-Pecht et al: Wide dynamic range APS star tracker, *Proc. Of SPIE* vol. 2654 *Solid State sensor array and CCD cameras* pp. 82-92(1996).

[9] E.R.Fossum: CMOS Image Sensors: Electronic Camera On a chip, *IEEE International Electron Devices Meeting Technical digest*, December 10-13, 1995, Washington D.C.

[10] E.R.Fossum: Active Pixel Sensors: Are CCD's dinosaurs? *Proc. of the SPIE Vol. 1900, Charge-Coupled Devices and solid State Optical sensors III* (1993).

[11] O. Yadid-Pecht et al: CMOS Active Pixel Sensor star Tracker with Regional Electronic Shutter, *IEEE Journal of solid State Circuits Vol. 32, Nit. 2*, February 1997.

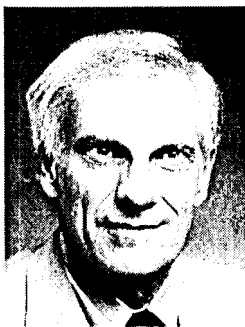
[12] Christian Buil: CCD Astronomy, *Willmann-Bell Inc., Virginia*, 1991.

## 8. BIOGRAPHIES

Dr. Carl Christian Liebe was born in Copenhagen in 1966. He received a MSEE in 1991 and a Ph.D. in 1994, both from the Department of Electrophysics, Technical University of Denmark. He was Research Assistant Professor at the Department of Automation, Technical University of Denmark 1995-1996. Since 1997, Dr. Liebe has been a member of the technical staff at the Jet Propulsion Laboratory, California Institute of Technology. His current research interests are new technologies and applications for autonomous attitude determination. He has authored/co-authored more than 20 papers.

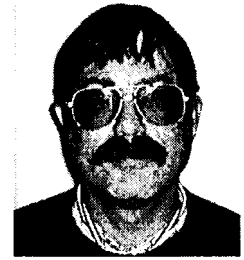


Dr. Edwin D. Dennison received his BA from Swarthmore College and Ph.D. from the University of Michigan with major in mathematics and astronomy. He has worked at the Sacramento Peak Observatory (New Mexico), the Mt. Wilson and Palomar Observatories and JPL. His special interest is the electronic measurement of light and associated data systems. At JPL he has worked on the ASTROS star tracker and supported (w) shuttle flights (Astro-1 and Ash-o-2). He has also worked on solar thermal concentrators for electric power generation, the star tracker for the Cassini mission and APS based star trackers. For these projects, he has been the cognizant engineer or engineering task lead. He has written and presented numerous papers on astronomical and spacecraft instrumentation.

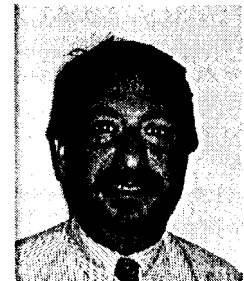


Dr. Bruce Hancock received the B.S. degree from the California Institute of Technology in 1979, and the M.S.E.E. and Ph.D. degrees from the University of California at Santa Barbara in 1982 and 1985, respectively. He joined the Jet Propulsion Laboratory, California Institute of Technology, Pasadena, in 1985, where his work included molecular beam epitaxy of III-V compounds and infrared sensor technology. More recently, he has been involved in

electronic parts reliability and radiation effects. He is currently a member of the Advanced Imager and Focal Plane Technology group, where is investigating radiation effects in active pixel sensors.



Dr. Robert C. Stirbl received his BSEE and MSEE from the City College of New York and Ph.D. at the Graduate Center of the City University of New York. He has taught at N.Y.U. School of Graduate Studies, Pratt Institute, City College of New York and was a Professor of Electrical Engineering at Manhattan College.



He is an experienced Project Manager; a recognized electro-optical system design expert and has 25 years of industrial experience. Dr. Stirbl has a proven track record of success for numerous industrial-consulting clients. He is a Member of the Advanced Imager and Focal Plane Technology Group at JPL. He is currently the system engineer/task manager for several BMDO and Air Force funded programs for advanced focal plane technology insertion into space systems. Dr. Stirbl holds 5 patents.

Dr. Bedabrata Pain was born in Calcutta, India in 1963. He received the Bachelor of Technology degree in Electronics and Electrical Communication Engineering in 1986 from the Indian Institute of Technology, Kharagpur, India, and the Masters and Ph.D. degree in Electrical Engineering at Columbia University, New York in 1989 and



1993 respectively. Since 1993 Dr. Pain has been with the Jet Propulsion Laboratory. Currently, he is a member of the Principal Engineering Staff, and heads the advanced imager and focal-plane technology group at JPL. His research interests include CMOS active pixel sensors, low-noise, low-power mixed analog/digital VLSI sensor & readout technology, and radiation detectors. Dr. Pain has received the Lcw Allen Award for Excellence in 1997 for his contribution to the field of CMOS active pixel sensors, and two NASA Achievement awards for his contributions to integrated imager technology in 1996. He has received several NASA certificates of recognition for his work relating to high-functionality CMOS APS, digital sensors, solid-state photon counting sensors, and infrared sensors. He has published over twenty-five technical papers, and holds several US patents in the field of integrated sensor technology. Dr. Pain is a member of the IEEE and the SPIE.